生物物理学报 2013 年 9 月 第 29 卷 第 9 期: 646-657
ACTA BIOPHYSICA SINICA Vol.29 No.9 Sep. 2013: 646-657

# Evolution and Function of Prokaryotic Dynamin-Like Proteins

GENG Dandan[1,2], Simon Cichello[3], ZHANG Shaoqiang[1], CHEN Yong[2]

*1. Institute of Computer and Information Engineering, Tianjin Normal University, Tianjin 300387, China;*
*2. National Laboratory of Biomacromolecules, Institute of Biophysics, Chinese Academy of Sciences, Beijing 100101, China;*
*3. School of Life Sciences, La Trobe University, Melbourne, Victoria 3086, Australia*

This work was supported by grants from the National Natural Science Foundation of China (61273228, 61103073), and the Natural Science Foundation of Tianjin Science and Technology Committee (11JCYBJC26600)
**Received:** Jul 28, 2013 **Accepted:** Sep 1, 2013
**Corresponding author:** ZHANG Shaoqiang, Tel: +86(22)23766027, E-mail: sqzhang@163.com
CHEN Yong, Tel: +86(10)64888521, E-mail: yongchen@tsinghua.edu.cn

**Abstract:** Membrane dynamics are essential for the numerous cellular processes in eukaryotic and prokaryotic cells. Membrane fusion and fission are often catalysed by large GTPases of the dynamin protein families in eukaryotic cells, however the mechanisms responsible in prokaryotes are yet to be investigated in depth. With new results of the structural and biochemical data of prokaryotic dynamin-like proteins (DLPs) becoming available, this review summarizes current knowledge regarding prokaryotic dynamins, and discusses their structural and functional properties. The mechanisms how DLPs are involved in lipid droplets (LDs) formation and fission are investigated, and highlighted as a potential research area of LD dynamics. Based on these understandings, a hypothetical model is then described and further research analysis proposed.

**Key Words:** Dynamin-like protein; Lipid droplet; Functional evolution; Protein domain; Membrane dynamics
**DOI:** 10.3724/SP.J.1260.2013.20146

## Introduction

Biological membranes dynamics are of vital importance for both eukaryotic and prokaryotic cells. The membrane dynamics are involved in many crucial processes as they can not only separate the cytoplasm, but also be related to sub-cellular compartmentalization[1,2]. Membrane fusion and fission events are usually catalysed by a super family known as dynamins, including the classical dynamins and DLPs that are ubiquitously distributed throughout animals, and plants species, but seldom in prokaryotes[3~6]. Classical dynamins and DLPs share similar modular domain architecture with a conserved GTPase domain, an α-helical stalk region and a membrane associated domain[7]. In eukaryotic cells, these large scale domain movements are reported to drive membrane dynamics such as vesicle scission[2], mitochondrial and endoplasmic reticulum (ER) fusion[8], as well as fusion of the mitochondrial outer and inner membranes[9,10]. Mutations in human DLPs are associated with various diseases[11~13], such as Alzheimer's and Parkinson's diseases[14], and also an apoptosis role in diabetic neuropathy in the dorsal root ganglia[15] indicating the functional importance of these proteins also in prokaryotes or uni-cellular *in vitro* cell lines as potential models of study for human disease.

Compared with eukaryotic DLPs, prokaryotic DLPs have long been neglected, since most bacteria lack internal membrane structures or organelles. The concept of bacterial dynamin-like protein (BDLP) was initially suggested in the report of the structure of a DLP from cyanobacterium *Nostoc punctiforme*[3]. Cryo-electron microscopy has provided further insight into the putative conformational re-arrangements that DLPs are needed to modulate membranes[16]. A recent publication showed for the first time that the prokaryotic DLPs might catalyze

membrane fusion, in addition to mitofusins using a biochemical method[17]. A DLP, DynA, was recently reported to be localized in inner membrane in *Bacillus subtilis*[18], consistent with what has been observed for the BLDP from *Nostoc punctiforme*[3]. However, the deletion of DynA had been shown to display no division phenotype for vegetative growing cells. Three DynA functional partners, Ynek, RNaseY and YwpG, had been also investigated by deleting a division protein MinJ in *Bacillus subtilis* that caused a dispersed distribution of DynA all over the cell inner membrane[18].

Recently, the discovery of LD organelle in *Rhodococcus jostii* RHA1 suggested new areas for prokaryotic membrane dynamics[19]. LD is an important and dynamic organelle that is encapsulated by a phospholipids monolayer[20,21]. LD is the only observed intracellular membranes of RHA1 and related to multiple cellular functions, such as lipid metabolism, signalling and protein degradation[19,22]. Interestingly, a DLP, ro_05488, was detected to be located on surface of LDs in RHA1 cells by proteomic analysis[19]. Furthermore, in a comparative transcriptomic study, PD630 cells were transferred from nutrient broth (NB) to mineral salt medium (MSM) cultures, which resulted in the enlargement of LD with concurrent and significantly differential expressions of DLPs[23]. These observations suggest DLPs may be related to the formation or membrane dynamics of LDs, thus indicating new functional roles of prokaryotic DLPs.

In this review, we systematically discuss the distribution of DLPs in bacteria and archaea. Protein domain and operon structures of DLPs are then reviewed to present a detailed evolutionary dynamics of these proteins. We also summarize current knowledge of structures, locations and functions of prokaryotic DLPs, and in particular their potential functions in LD dynamics. In culmination, this information provides a comprehensive model of how DLPs are involved in LD formation and fission.

## Origin and evolution of DLPs in RHA1

The first structure and location of a prokaryotic DLP ZP_00108538 was reported in a systematic analysis of *Nostoc punctiforme* in 2006[3]. Further research revealed that DLP ro_05488 was observed in a LD proteomic study of RHA1, with three other proteins ro_05469, ro_05470 and ro_05487 were found to share a similar sequence with ZP_00108538[19]. In our integrated omics study of LD dynamics in PD630, we identified four potential genes coding for DLPs including LPD02043, LPD02044, LPD02062 and LPD02063 with sequence length of 491, 562, 614 and 498 amino acids, respectively[23]. They are sequence similar with ZP_00108538 with E-value of 4.0E-11, 6.0E-04, 2.0E-08 and 3.0E-11, respectively. So far, prokaryotic DLPs have been predicted, but a systematic analysis of DLPs distribution in prokaryotes is still absent.

Initially, we performed a sequence blast with all sequenced prokaryotic genomes in the NCBI database by using these four proteins ro_05469, ro_05470, ro_05487 and ro_05488. In total 93, 82, 92 and 74 proteins were respectively detected with cut off 1.0E-03. Considering there are many redundant proteins existing among close species, we constructed a genome set of 146 genomes to enquire how many DLPs are distributed among genomes with certain evolutionary distance. A total of 146 genomes with maximal length were selected from each genus. The individual genus was defined as a relative evolutionary distance in the prokaryotic kingdom as previous described[24]. Using an E-value cut off of 1.0E-15, we detected 17, 13, 26 and 17 homologous genes in bacteria and archaea for the four identified potential genes respectively. The total 27 genomes and their genus annotations are shown in Table 1. As the gene ro_05487 is the most widely distributed protein (27 homologous) in these four proteins, we used it to construct a rooted maximum likelihood tree by using MEGA_5.1[25] to investigate the origin and evolution of the DLPs (Fig.1). We observed that the 27 homologous genes spanned 9 orders, including *Actinomycetales*, *Oscillatoriales*, *Chroococcales*, *Myxococcales*, *Thermoanaerobacterales*, *Methanomicrobiales*, *Methylococcales*, *Clostridiales* and *Syntrophobacterales*, but are not uniformly distributed. Specifically, most of the orders contained only one or two genera, but *Actinomycetales* contained 16 genera. The four proteins are displayed different distributions. The protein ro_05470, ro_05469 and ro_05488 are only observed in a few of the 27 genera. For example, ro_05469 and ro_05488 are found in 18 genera, while ro_05470 is found in 14 genera. Considering that the above protein phylogenetic profile is not a standard description of species evolutionary distance, we then mapped the four proteins on the phylogenetic lineages presented by NCBI genome database based on 16sRNA analysis (Fig.2)[26]. It is obviously that the cluster A and B (Fig.2) contain only the gene ro_05487, while the others contain at least three potential coding genes. These two types of phylogenetic analysis both indicate that ro_o5487 is most evolutionary conserved than other three proteins.

Table 1 The 27 genomes and their taxonomic annotations
表 1 27 个基因组及它们的物种分类注释

| Order name | Genus name | Strain name | NCBI_ID |
|---|---|---|---|
| *Actinomycetales* | *Rhodococcus* | *Rhodococcus jostii* RHA1 | NC_008268 |
| | | | NC_008269 |
| | | | NC_008270 |
| | | | NC_008271 |
| | *Amycolicicoccus* | *Amycolicicoccus subflavus* DQS3-9A1 | NC_015564 |
| | | | NC_015560 |
| | | | NC_015561 |
| | *Gordonia* | *Gordonia polyisoprenivorans* VH2 | NC_016906 |
| | | | NC_016907 |
| | *Nocardia* | *Nocardia farcinica* IFM 10152 | NC_006361 |
| | | | NC_006362 |
| | | | NC_006363 |
| | *Mycobacterium* | *Mycobacterium smegmatis* str. MC2 155 | NC_008596 |
| | *Pseudonocardia* | *Pseudonocardia dioxanivorans* CB1190 | NC_015312 |
| | | | NC_016601 |
| | | | NC_015313 |
| | | | NC_015314 |
| | *Blastococcus* | *Blastococcus saxobsidens* DD2 | NC_016943 |
| | *Saccharopolyspora* | *Saccharopolyspora erythraea* NRRL 2338 | NC_009142 |
| | *Saccharomonospora* | *Saccharomonospora viridis* DSM 43017 | NC_013159 |
| | *Actinosynnema* | *Actinosynnema mirum* DSM 43827 | NC_013093 |
| | *Microlunatus* | *Microlunatus phosphovorus* NM-1 | NC_015635 |
| | *Salinispora* | *Salinispora arenicola* CNS-205 | NC_009953 |
| | *Amycolatopsis* | *Amycolatopsis mediterranei* U32 | NC_014318 |
| | *Frankia* | *Frankia* sp. EuI1c | NC_014666 |
| | *Streptosporangium* | *Streptosporangium roseum* DSM 43021 | NC_013595 |
| | | | NC_013596 |
| | *Stackebrandtia* | *Stackebrandtia nassauensis* DSM 44728 | NC_013947 |
| *Methanomicrobiales* | *Methanoregula* | *Methanoregula boonei* 6A8 | NC_009712 |
| | *Methanospirillum* | *Methanospirillum hungatei* JF-1 | NC_007796 |
| *Myxococcales* | *Sorangium* | *Sorangium cellulosum* 'So ce 56' | NC_010162 |
| | *Haliangium* | *Haliangium ochraceum* DSM 14365 | NC_013440 |
| *Clostridiales* | *Syntrophothermus* | *Syntrophothermus lipocalidus* DSM 12680 | NC_014220 |
| | *Thermincola* | *Thermincola potens* JR | NC_014152 |
| *Oscillatoriales* | *Trichodesmium* | *Trichodesmium erythraeum* IMS101 | NC_008312 |
| *Chroococcales* | *Cyanothece* | *Cyanothece* sp. PCC 7822 | NC_014501 |
| | | | NC_014503 |
| | | | NC_014504 |
| | | | NC_014533 |
| | | | NC_014535 |
| | | | NC_014534 |
| | | | NC_014502 |
| *Thermoanaerobacterales* | *Carboxydothermus* | *Carboxydothermus hydrogenoformans* Z-2901 | NC_007503 |
| *Methylococcales* | *Methylococcus* | *Methylococcus capsulatus* str. Bath | NC_002977 |
| *Syntrophobacterales* | *Syntrophobacter* | *Syntrophobacter fumaroxidans* MPOB | NC_008554 |

The IDs of each strain include the main chromosome and plasmids, and taxonomic annotation is downloaded from NCBI database
每个菌株中主染色体和质粒的编号及物种分类注释信息均来源于 NCBI 数据库

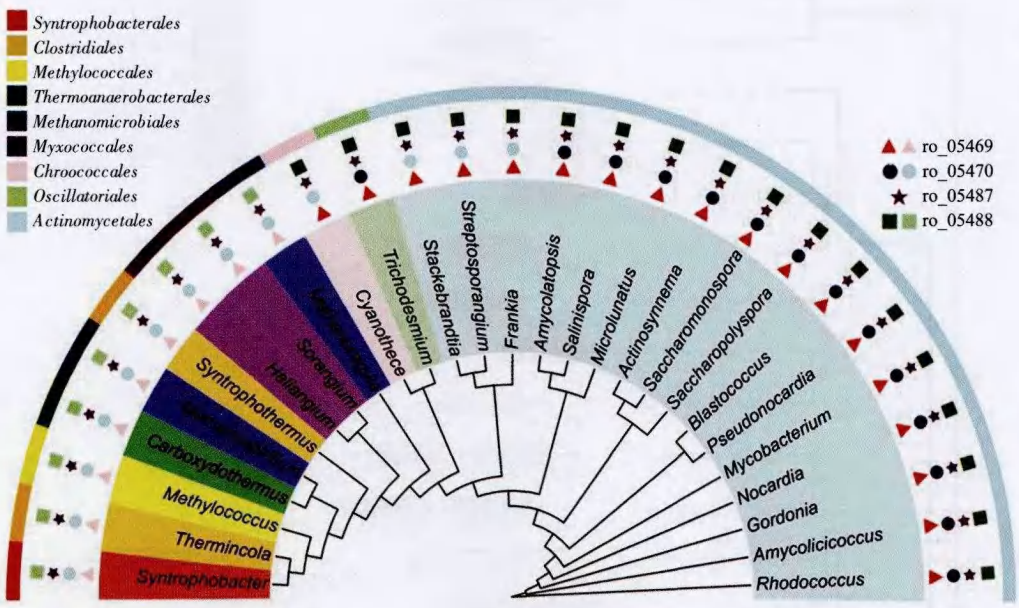


Fig.1 Phylogenetic analysis of RHA1 DLP family The rooted maximum likelihood tree was constructed by using 26 homology genes of ro_05487 of *Rhodococcus jostii* RHA1. The tree is rooted on ro_05487 (*Rhodococcus*) and plotted by MEGA_5.1. The genera in each of nine orders are marked with same colour. The four potential coding genes are represented by different symbols, whereby dark colour means existence and light colour means inexistence

图 1 RHA1 中动力蛋白家族的进化分析 利用 MEGA_5.1 软件，分析了 RHA1 中的基因 ro_05487 及其 26 个同源基因的最大似然有根进化树 (以 ro_05487 为根)。图中的 27 个属共可划分为九个目。图例中的四种图形分别代表动力蛋白家族的四个基因，深色表示该基因存在于对应的物种中，浅色表示在该物种中没有被检测到

In RHA1, protein ro_05469 and ro_05470 are constructed as an operon, while ro_05487 and ro_05488 are constructed another. Since all genes in an operon are usually co-regulated and thus involved in same biological pathways, we further examined whether these operon structures or co-regulators are evolutionary conserved. The best hit proteins of these four proteins in all 27 genera are predicted by using the BLAST program [27]. Interestingly, it was observed that in nine genera (Cluster A and B, Fig.2) there was only one protein located, whereas no related operon structure was observed. Moreover, the operon structure was found in other genera but the copy number was different. In the genera *Nocardia* and *Rhodococcus*, there were two separated operons found, while there was only one operon found in the other genera (Fig.2). A similar operon structure was also detected in PD630, where LPD02043 and LPD02044 were constructed as an operon, and LPD02062 and LPD02063 also constructed another operon. Furthermore, we found that only LPD02062 and LPD02063 are expressed, but the expressions of LPD02043 and LPD02044 are not detected [23], suggesting that LPD02043 and LPD02044 may be the only duplicated pairs of LPD02062 and LPD02063. These results show that the evolutionary dynamics of prokaryotic DLPs are not observed in single protein but rather as a regulatory unit.

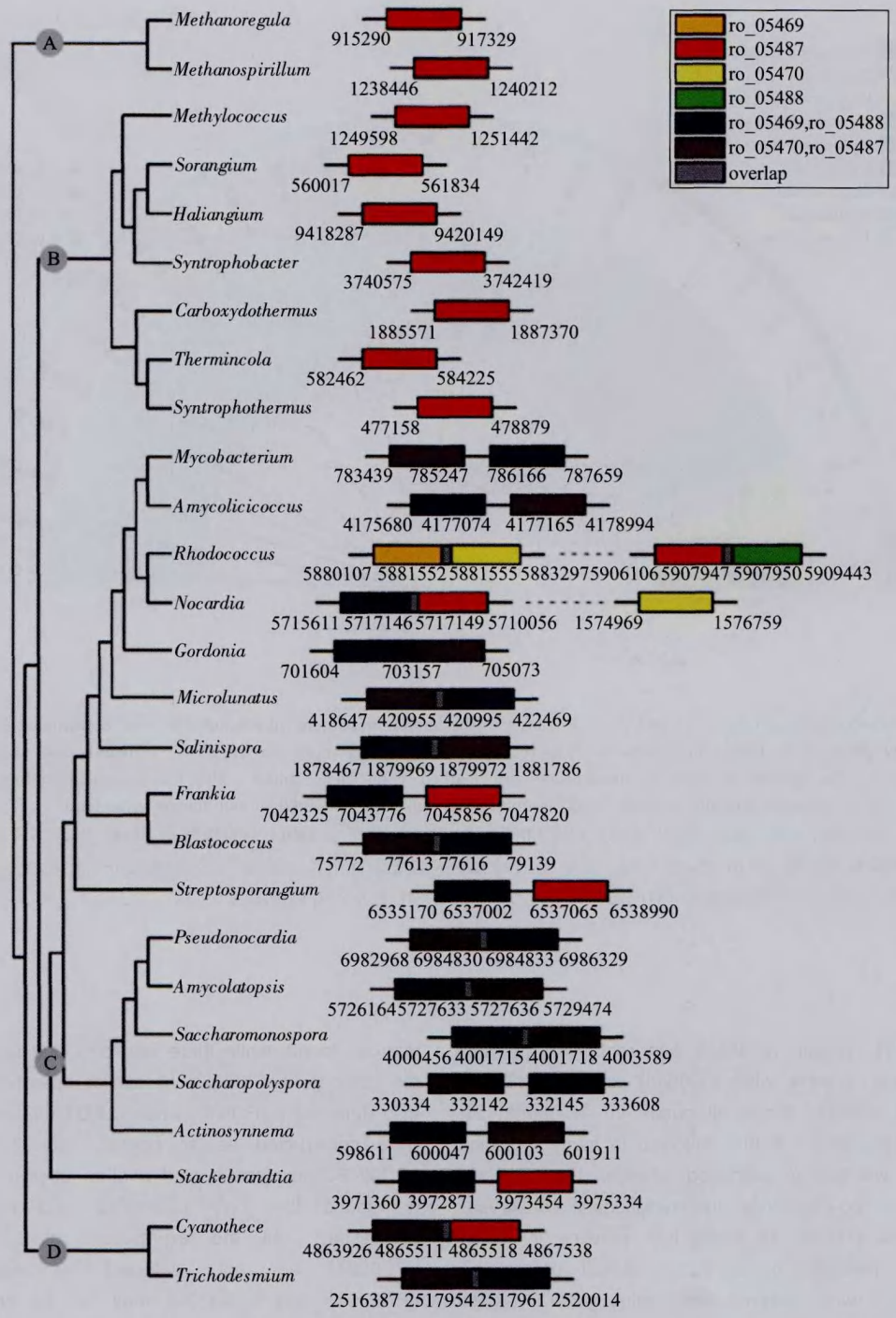


Fig.2 Evolutionary tree based on the 16sRNA The tree of 27 genomes is drew based on NCBI evolutionary linkage. The genes that most similar to two query genes are marked in blue and purple. Grey shows the overlap of protein locations. Four groups are clustered and annotated A, B, C and D. Data under the gene structure describe the starting and ending positions. "..." illustrates that the genes are located in far distance along genome

**图 2 基于 16sRNA 构建的系统进化树** 图中 27 个物种的进化树是依据 NCBI 中的物种进化关系构建的。如果两个基因的最佳匹配基因相同，则分别用蓝色或紫色矩形表示。灰色矩形表示重叠的基因片段。图中的进化树可主要划分为 A、B、C 和 D 四个分支。各基因片段下面对应的数字分别代表该基因片段的起始和终止位置。省略号表示两个基因片段在染色体上的距离间隔较远

## Structure and evolution of the protein domains in DLPs

Recently published structural data of full-length classical dynamins and DLPs have shown that all members of the dynamins follow the same architecture in eukaryotic cells[28]. The traditional view was that members of the dynamins contain at minimum three functional domains a GTPase domain, a middle domain and a GTPase effector domain[2]. The later crystal structure of the BDLP from *Nostoc punctiforme* provides a new view of prokaryotic DLPs 3-D structures [3]. The electron microscopy data of the 3.1 Å and 3.0 Å resolution of a GDP-associated and also a nucleotide-free state show that dynamins consist of a GTPase head, a four helix neck and trunk bundle, and a tip domain. In details, the predicted middle domain and GTPase effector domain do not form discrete entities, but are part of four helix bundles and connected to the GTPase domain via a linker.

A key trait of classical dynamins and DLPs is their capacity of GTP binding and hydrolysing that is performed by the GTPase head (also called GTP/$Mg^{2+}$ binding site) according to NCBI conserved domain database[1,29]. We further investigated the sequence conserved sites in this GTPase head to identify potential functional conserved sites. Based on the NCBI conserved domain database and Pfam database [30], we first obtained the conserved and well-characterized motifs of the four RHA1 proteins ro_05469, ro_05470, ro_05487 and ro_05488 (Fig.3). Visually, all of the four potential coding genes contain seven sub-motifs as the Switch I region, Switch II region and G1~G5 box in the GTP/$Mg^{2+}$ binding region. To further investigate the domain architecture and the conservative property of these functional motifs, we performed the multi-sequence alignment of ro05487 against 26 other proteins (Fig.4). Highly conserved motif sequences are predicted such as G1 box

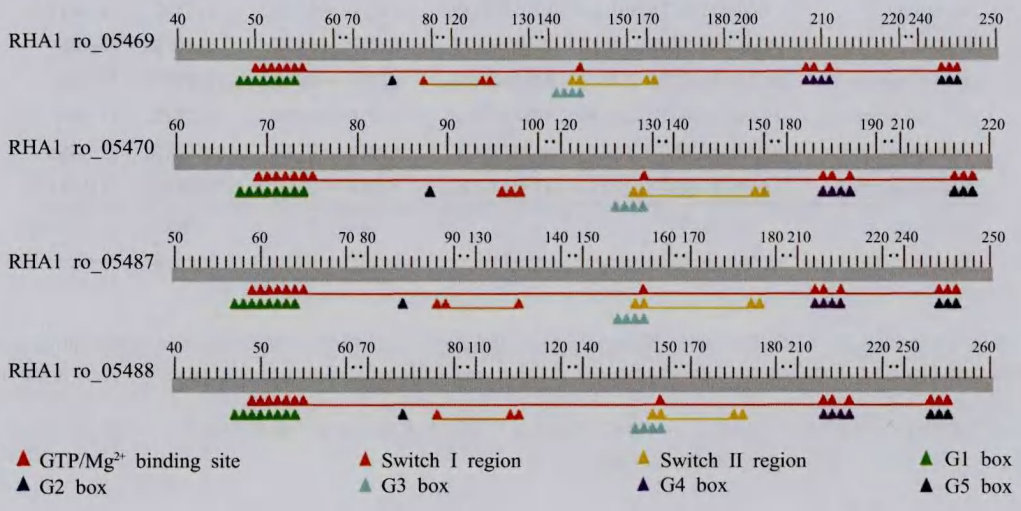


Fig.3 Domain structures of DLPs in RHA1 The functional motifs are predicted by using NCBI conserved domain database. GTP/$Mg^{2+}$ binding site (red) is the main functional region, including seven sub-motifs as Switch I region (orange), Switch II region (yellow), G1 box (green), G2 box (blue), G3 box (cyan), G4 box (purple) and G5 box (dark blue). To each protein, each scale in the graphic represents relative positions of these motifs

**图 3 RHA1 中的动力蛋白域结构** 基于 NCBI 中的保守域数据库，在 RHA1 的四个蛋白中总共预测到八个功能域。GTP/$Mg^{2+}$ 结合位点 (红色) 为主要功能域，它包含 Switch I (橙色)、Switch II (黄色)、G1 (绿色)、G2 (蓝色)、G3 (青色)、G4 (紫色) 和 G5 (深蓝色) 七个子功能域。图中每一个刻度代表一个碱基，上面的数字表示该碱基在对应基因片段中的位置

| | G1 | G2 | G3 | G4 | G5 |
|---|---|---|---|---|---|
| *Carboxydothermus* | LAVLGQFKRGKSTFINALLG | VLPLTAVPIF | LIDTP——GIGST | ILNKVDY | FGVSARL |
| *Methanospirillum* | LAILGQFKRGKSTFLNALLG | VIPLTAVPTL | LIDTP——GVGST | LLNKIDY | YPVSAKQ |
| *Syntrophobacter* | LVVVGQFKRGKTYLINALMG | VVPLTSIVTV | LIDTP——GVGSV | LLNKIDH | YPVSAKL |
| *Thermincola* | LVVLGQFKRGKTTFINSLLG | VVPLTSIVTV | LIDTP——GVGSI | ILNKIDY | FPLSAKL |
| *Methylococcus* | VLTVGQFKRGKTSLINALLG | AVPLTSVVTV | IVDTP——GVGSV | LLNKIDI | FPISARE |
| *Amycolatopsis* | VYVVGEFKQGKSSLINALLT | DDIATAVPTV | LVDTP——GVGGL | VLTKIDL | IAVSSEL |
| *Salinispora* | VVVVGEFKKGKSSLVNALVG | DGPATAVPTQ | LVDTP——GVGGL | VMTKTDF | MAVSSTL |
| *Rhodococcus* | IVVVGPLKQGKSQFVNSLLN | DDETTAIPTV | LVDTP——GVGGA | LISKTDL | IPISSVL |
| *Amycolicicoccus* | VAVVGELKQGKSQLVNSLIN | DDEATAVPTQ | LIDTP——GVGGH | IVTKTDL | LPVSALL |
| *Gordonia* | IVVVGNLKQGKSQFVNALLN | DDESTAVPTL | VIDTP——GVGGH | LFTKTDL | LPVSSTM |
| *Nocardia* | IVVAGLLGQGKSRLVNALMN | DDTTTTVATV | LVDTP——GVGGQ | MLTKTDL | LPVSALL |
| *Mycobacterium* | VVIAGQLKQGKSQLLNSLLN | DDESTVLATV | FVDTP——GVGGH | VATKTDL | IPASSVL |
| *Actinosynnema* | VLVVGESKQGKSQLVNALIN | DDVTTAVPTF | LIDTP——GTGDP | VLTKTDL | LPVSSAL |
| *Saccharomonospora* | VVVLGGSGQGKSQLLNGLLG | DDLTTTVPTV | LIDTPPCGTDGDH | VLTKTDL | FPVSSAL |
| *Saccharopolyspora* | VLIVGESKQGKSELVNAIVN | EDVTTVVPTL | LMDTP——GVGSV | VQPKIDV | FPVSSVV |
| *Blastococcus* | VLVVGEPKQGKSQLVNALVG | DDVATVVPTV | LVDTP——GVGGI | AVTKTDV | FPVSASL |
| *Pseudonocardia* | VLIVGEFKQGKSQLVNALVN | DDIATSVPTV | LVDTP——GVGGL | VVTKTDL | FPVSSTL |
| *Microlunatus* | VVFCGQFKVGKSTMINALLQ | ADVVTAVPTV | VVDTP——GVGGL | VVTKTDL | FAVSSFL |
| *Cyanothece* | VVVCGEFKQGKSSLINAFLN | TDITTNLVST | LVDTP——GVGSL | VVTKIDA | IPISSRA |
| *Trichodesmium* | VVVCGEFKEGKSSLINALLK | ADIATGIVST | LVDTP——GVGGL | VVTKIDS | VPVSSHN |
| *Haliangium* | LVVLGEFNHGKSSFVNALLG | ITPTTATINH | LVDTP——GVNDL | VLGKSDL | LVPEPAL |
| *Sorangium* | LVVVGEFNHGKTTFVNALLG | VTPTTAVIHH | LVDTP——GVNDL | VVTKRDI | LVKSPVV |
| *Frankia* | VVVVGEKKRGKSSLLNALLG | VDVATNVHLT | LVDTP——GVGGL | VLAQIDK | FPVSSRF |
| *Stackebrandtia* | MVIVGETKRGKSSLTNALIG | AAVATSSYLE | LIDTP——GVGGL | ALTKTDA | FPVSSRL |
| *Streptosporangium* | IVVAGAQKRGKSRLLNTLVG | ADVATNCFLS | LLDTP——GVDSL | VLTKVED | IPVSSKL |
| *Syntrophothermus* | VAVLGSFKAGKSSFLNSLIG | NIPVTSVITR | LVDTP——GIGSV | VITKVDL | FPIYRHS |
| *Methanoregula* | IAVFGRVSSGKSSLLNAIIG | VTPVTAVPTR | FVDTP——GLGSL | LLSKADL | LVKSALD |
| conserved motifs | GxxxxGKS | T | Dxx G | NKxD | SAK |
| consensus aa | ——G—K-GKS——N-L— | ——T—— | L-DTP——GVG— | —K-D- | —S— |

Fig.4 Conserved sequences of DLP motifs Multi-sequence alignment of ro_05487 with other best hit 26 proteins shows five well characterized motifs. Critical residues are highlighted in bold and consensus sequences are presented with a cut off of 80% identity

**图 4 动力蛋白的保守功能域序列** 利用基因 ro_05487 与其他 26 个基因的多序列比对，分别得到了 5 个功能域中保守的功能位点(粗体)。最下方的序列给出了保守性超过 80%的氨基酸位点

(GxxxxGK[ST]), G2 box (T) and a less conserved motif G3 box (DxxG). In addition, GTP-utilizing enzymes share the feature G4 box ([NT]KxD)[31]. Additional contacts to the nucleotide are made by residues similar to the G5 box (SA[KL])[1,32]. Consensus sequences of these motifs further show some additional conserved sites existed, indicating that these sites may be also involved in some potential functions. A distribution summary of these motifs among 27 genes is shown in Table 2. It is observed that most of these motifs exist among the 27 homologous genes, but Switch I region, G1 box and G2 box are frequently absent.

Table 2 Distributions of the motifs in 27 proteins
表 2 27 个蛋白中功能域的分布

| Genus Name | GTP/$Mg^{2+}$ binding site | Switch I | Switch II | G1 | G2 | G3 | G4 | G5 |
|---|---|---|---|---|---|---|---|---|
| *Carboxydothermus* | Y | Y | Y | Y | Y | Y | Y | Y |
| *Methanospirillum* | Y | Y | Y | Y | Y | Y | Y | Y |
| *Syntrophobacter* | Y | Y | Y | Y | Y | Y | Y | Y |
| *Thermincola* | Y | Y | Y | Y | Y | Y | Y | Y |
| *Methylococcus* | Y | Y | Y | Y | Y | Y | Y | Y |
| *Amycolatopsis* | Y | Y | Y | Y | Y | Y | Y | Y |
| *Salinispora* | Y | Y | Y | Y | Y | Y | Y | Y |
| *Rhodococcus* | Y | Y | Y | Y | Y | Y | Y | Y |
| *Amycolicicoccus* | Y | Y | Y | Y | Y | Y | Y | Y |
| *Gordonia* | Y | Y | Y | Y | Y | Y | Y | Y |
| *Nocardia* | Y | N | Y | N | N | Y | Y | Y |
| *Mycobacterium* | Y | Y | Y | Y | Y | Y | Y | Y |
| *Actinosynnema* | Y | Y | Y | Y | Y | Y | Y | Y |
| *Saccharomonospora* | Y | N | Y | N | N | Y | Y | Y |
| *Saccharopolyspora* | Y | Y | Y | Y | Y | Y | Y | Y |
| *Blastococcus* | Y | N | Y | N | N | Y | Y | Y |
| *Pseudonocardia* | Y | Y | Y | Y | Y | Y | Y | Y |
| *Microlunatus* | Y | N | Y | Y | N | Y | Y | Y |
| *Cyanothece* | Y | Y | Y | Y | Y | Y | Y | Y |
| *Trichodesmium* | Y | Y | Y | Y | Y | Y | Y | Y |
| *Haliangium* | Y | Y | Y | Y | Y | Y | Y | Y |
| *Sorangium* | Y | Y | Y | Y | Y | Y | Y | Y |
| *Frankia* | Y | N | Y | N | N | Y | Y | Y |
| *Stackebrandtia* | Y | Y | Y | Y | Y | Y | Y | Y |
| *Streptosporangium* | Y | Y | Y | Y | Y | Y | Y | Y |
| *Syntrophothermus* | Y | Y | Y | Y | Y | Y | Y | Y |
| *Methanoregula* | Y | Y | Y | Y | Y | Y | Y | Y |

All eight motifs are predicted in 27 proteins (each protein for one genus) by using NCBI conserved domain database. "Y" means existence and "N" means inexistence
基于 NCBI 中的保守功能域数据库，统计了 27 个蛋白中的 8 个功能域分布。“Y”表示该功能域存在于对应的物种中，“N”表示不存在

## Localization and partner of DLPs

To observe localization of DLPs *in vivo*, the translational fusion of BDLP and green fluorescent protein (GFP) was constructed and expressed in wild type *Nostoc punctiforme*[3]. The GFP fusions localized to the cell periphery was clearly observed by confocal fluorescence microscopy. In addition, some of the GFP fusions were also observed to be localized to the cell septum and presented ring-like structures.

Although the BDLPs pre-dominantly localized to the cell membrane, recent research revealed that the location may be regulated or interacted with the interaction of other proteins. In *Bacillus subtilis*, Frank et al[18] showed that MinJ, which is a topological determinant protein during cell division, may play an important role in controlling

location of the DynA, as DynA was no longer located on the membrane of the MinJ mutated cells. Furthermore, three proteins YneK, RNaseY and YwpG were detected to be co-localized with DynA, suggesting that they may be associated with DynA in modelling membrane dynamics.

## Hypothetical functions of DLPs in membrane dynamics

Although structural and biochemical information of BDLPs are available, the function of these proteins is not at present clearly defined. According to previous studies, various hypotheses have been presented, but can be summarised into two major categories. Firstly, BDLPs may facilitate bacteria cell release of membrane vesicles into the environment [33,34]. In bacteria, large membrane vesicles are derived mainly from constricted division septa and small membrane vesicles occur most frequently at locations distributed along the cell body. During these processes, endosomal sorting complex required for transport (ESCRT-III) homologues surround the site of nascent membrane formation and cleave membranes from the inside of a cell. Then BDLPs catalyze the disassembly of ESCRT-III homologues and membrane vesicle release occurs. Although the phenomenon of membrane vesicle release has been recognized for decades, how BDLPs assist in this dynamic process remains unclear yet. Secondly, BDLPs could function in catalysing membrane fusion in the later stage of cytokinesis [1]. With the aid of protein-protein contacts or attraction of negatively charged phospholipids, the *Bacillus subtilis* protein DynA is recruited at the site of septation, presenting ring structure. Under the trans action of DynA, the septal membrane is incurved and fused ultimately. However, direct supporting evidence of this proposed model was not provided in current publications.

Since most bacteria lack internal membrane structures or organelles, the emergence of LDs in some prokaryotes presents a new paradigm to the DLPs in modelling membrane dynamics. In an earlier LD proteomic study, a DLP ro_05488 was detected on surface of LDs in RHA1 cells [19]. This is further confirmed by the identification of two DLPs LDP_02062 and LDP_02063 on the LD surface in PD630. Interestingly, when the sizes of LDs are enlarged using MSM instead of NB growth medium, the expressions of LDP_02062 and LDP_02063 are observed to be significantly altered by comparative transcriptomic analysis [23]. Since the DLPs are involved in vesicle scission in eukaryotic cells [35], these evidences strongly suggest DLPs may be related to the formation and the membrane dynamics of LDs. Based on the above analysis, we presented a hypothetical model to explain how the DLPs are involved in LD membrane dynamics (Fig.5). Firstly, during TAG accumulation, the inner membrane may be curved with the collaboration of LD structural like proteins. This process results in LD budding towards the cytoplasm. Secondly, the DLPs locate at the neck of the LD, and aid in disengagement by the cooperation of an adapter or partner proteins. Thirdly, a fission process may also occur, and as a result, a mature LD is divided into two small LDs with collaboration of DLPs. The formation and fission process of LDs had been observed in budding yeast, but detailed mechanisms are absent [36,37]. This hypothetical model may present a new direction to the studies of LD formation and fission.

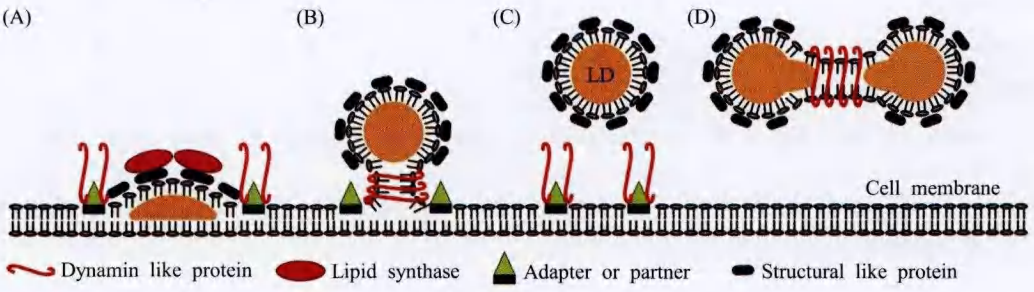


Fig.5 Hypothetical model of DLPs in LD dynamics (A) TAG accumulation and budding. During the budding process, TAG synthesis proteins may play a key role in TAG synthesis and accumulation in the lipid bilayer, resulting in membrane curved. (B,C) Disengagement. DLPs locate at the neck of the LD and aid in disengagement by the cooperation of adapter or partner proteins. (D) Fission. A mature LD may be divided into two small LDs with help of DLPs

图 5 动力蛋白参与脂滴动态变化过程的假说模型 (A) TAG 的累积和凸起。在此过程中，TAG 合成蛋白可能起着关键作用，它负责在磷脂双分子层中 TAG 的合成和累积，并最终导致细胞膜发生弯曲，形成凸起。(B,C) 脱离。动力蛋白位于脂滴凸起形成的脖颈处，并与其他蛋白相互作用，共同帮助脂滴脱离细胞内膜。(D) 分裂。一个成熟的脂滴可能在动力蛋白的帮助下分裂为两个小脂滴

## Conclusions

In recent years, large amounts of structural and biochemical data have been disseminated and presented regarding the comprehensive analysis of classical dynamins or how DLPs modulate biological membranes. In this review, we investigated the DLPs in RHA1 and identified four potential genes coding for DLPs. According to the analysis of both the origin and evolution, we find that the DLPs are evolutionarily derived from *Actinomycetales* and can even be traced to archaea. The operon structures may be constructed by duplication events, which have occurred occasionally during the evolutionary process[24]. Based on the summary of prior knowledge, we dissected the structure and potential functions of the DLPs. We highlighted that DLPs may be related to the formation and dynamics of LDs, which have been identified as an important organelle not just for lipid storage but also energy metabolism regulation. In PD630, the discovery of DLPs on LD surface and also the companion of differential expression in LD morphological dynamics, suggest that DLPs may play important roles in the LD formation and fission processes. Thus, the formation ratio of LD may be affected by controlling DLPs expression. Considering PD630 is an oleaginous bacterium with an application for biofuel production[38-40], further research of DLPs may be advantageous not only to investigate the formation of LD organelle, but also improve biofuel production by accelerating TAG accumulation and storage in LD.

## Acknowledgements

The authors would like to thank all lab members for useful discussions.

## References:

1. Bramkamp M. Structure and function of bacterial dynamin-like proteins. *Biol Chem*, 2012, 393(11): 1203~1214
2. Praefcke GJ, McMahon HT. The dynamin superfamily: Universal membrane tubulation and fission molecules? *Nat Rev Mol Cell Biol*, 2004, 5(2): 133~147
3. Low HH, Lowe J. A bacterial dynamin-like protein. *Nature*, 2006, 444(7120): 766~769
4. Yang Y, Glynn JM, Olson BJ, Schmitz AJ, Osteryoung KW. Plastid division: Across time and space. *Curr Opin Plant Biol*, 2008, 11(6): 577~584
5. Ferguson SM, De Camilli P. Dynamin, a membrane-remodelling GTPase. *Nat Rev Mol Cell Biol*, 2012, 13(2): 75~88
6. Pucadyil TJ. Dynamic remodeling of membranes catalyzed by dynamin. *Curr Top Membr*, 2011, 68: 33~47
7. Prakash B, Praefcke GJ, Renault L, Wittinghofer A, Herrmann C. Structure of human guanylate-binding protein 1 representing a unique class of GTP-binding proteins. *Nature*, 2000, 403(6769): 567~571
8. Byrnes LJ, Sondermann H. Structural basis for the nucleotide-dependent dimerization of the large G protein atlastin-1/SPG3A. *Proc Natl Acad Sci USA*, 2011, 108(6): 2216~2221
9. Santel A, Fuller MT. Control of mitochondrial morphology by a human mitofusin. *J Cell Sci*, 2001, 114 (Pt 5): 867~874
10. Meeusen S, DeVay R, Block J, Cassidy-Stone A, Wayson S, McCaffery JM, Nunnari J. Mitochondrial inner-membrane fusion and crista maintenance requires the dynamin-related GTPase Mgm1. *Cell*, 2006, 127(2): 383~395
11. Faelber K, Gao S, Held M, Posor Y, Haucke V, Noe F, Daumke O. Oligomerization of dynamin superfamily proteins in health and disease. *Prog Mol Biol Transl Sci*, 2013, 117: 411~443
12. Durieux AC, Prudhon B, Guicheney P, Bitoun M. Dynamin 2 and human diseases. *J Mol Med (Berl)*, 2010, 88(4): 339~350
13. Reddy PH, Reddy TP, Manczak M, Calkins MJ, Shirendeb U, Mao P. Dynamin-related protein 1 and mitochondrial fragmentation in neurodegenerative diseases. *Brain Res Rev*, 2011, 67(1-2): 103~118
14. Ranieri M, Brajkovic S, Riboldi G, Ronchi D, Rizzo F, Bresolin N, Corti S, Comi GP. Mitochondrial fusion proteins and human diseases. *Neurol Res Int*, 2013, 2013: 293893
15. Leinninger GM, Backus C, Sastry AM, Yi YB, Wang CW, Feldman EL. Mitochondria in DRG neurons undergo hyperglycemic mediated injury through Bim, Bax and the fission protein Drp1. *Neurobiol Dis*, 2006, 23(1): 11~22
16. Low HH, Sachse C, Amos LA, Lowe J. Structure of a bacterial dynamin-like protein lipid tube provides a mechanism for assembly and membrane curving. *Cell*, 2009, 139(7): 1342~1352
17. Burmann F, Ebert N, van Baarle S, Bramkamp M. A bacterial dynamin-like protein mediating nucleotide-independent membrane fusion. *Mol Microbiol*, 2011, 79(5): 1294~1304
18. Burmann F, Sawant P, Bramkamp M. Identification of interaction partners of the dynamin-like protein DynA from *Bacillus subtilis*. *Commun Integr Biol*, 2012, 5(4): 362~369
19. Ding Y, Yang L, Zhang S, Wang Y, Du Y, Pu J, Peng G, Chen Y, Zhang H, Yu J, Hang H, Wu P, Yang F, Yang H, Steinbuchel A, Liu P. Identification of the major functional proteins of prokaryotic lipid droplets. *J Lipid Res*, 2012, 53(3): 399~411
20. Fujimoto T, Ohsaki Y, Cheng J, Suzuki M, Shinohara Y. Lipid droplets: A classic organelle with new outfits. *Histochem Cell Biol*, 2008, 130(2): 263~279
21. Farese RV Jr, Walther TC. Lipid droplets finally get a little R-E-S-P-E-C-T. *Cell*, 2009, 139(5): 855~860
22. Murphy DJ. The biogenesis and functions of lipid bodies in animals, plants and microorganisms. *Prog Lipid Res*, 2001, 40(5): 325~438
23. Chen Y, Ding Y, Yang L, Yu J, Liu G, Wang X, Zhang S,

Yu D, Song L, Zhang H, Zhang C, Huo L, Huo C, Wang Y, Du Y, Zhang H, Zhang P, Na H, Xu S, Zhu Y, Xie Z, He T, Zhang Y, Wang G, Fan Z, Yang F, Liu H, Wang X, Zhang X, Zhang MQ, Li Y, Steinbüchel A, Fujimoto T, Cichello S, Yu J, Liu P. Integrated omics study delineates the dynamics of lipid droplets in *Rhodococcus opacus* PD630. *Nucleic Acids Res*, 2013, DOI: 10.1093/nar/gkt932

24. Chen Y, Yang L, Ding Y, Zhang S, He T, Mao F, Zhang C, Zhang H, Huo C, Liu P. Tracing evolutionary footprints to identify novel gene functional linkages. *PLoS One*, 2013, 8(6): e66817
25. Hall BG. Building phylogenetic trees from molecular data with MEGA. *Mol Biol Evol*, 2013, 30(5): 1229~1235
26. Pruitt KD, Tatusova T, Klimke W, Maglott DR. NCBI reference sequences: Current status, policy and new initiatives. *Nucleic Acids Res*, 2009, 37(Database issue): D32~36
27. Ye Y, Wei B, Wen L, Rayner S. BlastGraph: A comparative genomics tool based on BLAST and graph algorithms. *Bioinformatics*, 2013, DOI: 10.1093/bioinformatics/btt553
28. Ford MG, Jenni S, Nunnari J. The crystal structure of dynamin. *Nature*, 2011, 477(7366): 561~566
29. Marchler-Bauer A, Zheng C, Chitsaz F, Derbyshire MK, Geer LY, Geer RC, Gonzales NR, Gwadz M, Hurwitz DI, Lanczycki CJ, Lu F, Lu S, Marchler GH, Song JS, Thanki N, Yamashita RA, Zhang D, Bryant SH. CDD: Conserved domains and protein three-dimensional structure. *Nucleic Acids Res*, 2013, 41(Database issue): D348~352
30. Punta M, Coggill PC, Eberhardt RY, Mistry J, Tate J, Boursnell C, Pang N, Forslund K, Ceric G, Clements J, Heger A, Holm L, Sonnhammer EL, Eddy SR, Bateman A, Finn RD. The Pfam protein families database. *Nucleic Acids Res*, 2012, 40(Database issue): D290~301
31. Leipe DD, Wolf YI, Koonin EV, Aravind L. Classification and evolution of P-loop GTPases and related ATPases. *J Mol Biol*, 2002, 317(1): 41~72
32. Niemann HH, Knetsch ML, Scherer A, Manstein DJ, Kull FJ. Crystal structure of a dynamin GTPase domain in both nucleotide-free and GDP-bound forms. *EMBO J*, 2001, 20(21): 5813~5821
33. Deatherage BL, Lara JC, Bergsbaken T, Rassoulian Barrett SL, Lara S, Cookson BT. Biogenesis of bacterial membrane vesicles. *Mol Microbiol*, 2009, 72(6): 1395~1407
34. Deatherage BL, Cookson BT. Membrane vesicle release in bacteria, eukaryotes, and archaea: A conserved yet underappreciated aspect of microbial life. *Infect Immun*, 2012, 80(6): 1948~1957
35. van der Bliek AM, Meyerowitz EM. Dynamin-like protein encoded by the *Drosophila shibire* gene associated with vesicular traffic. *Nature*, 1991, 351(6325): 411~414
36. Dalhaimer P. Lipid droplet organelle distribution in populations of dividing cells studied by simulation. *Phys Biol*, 2013, 10(3): 036007
37. Long AP, Manneschmidt AK, VerBrugge B, Dortch MR, Minkin SC, Prater KE, Biggerstaff JP, Dunlap JR, Dalhaimer P. Lipid droplet de novo formation and fission are linked to the cell cycle in fission yeast. *Traffic*, 2012, 13(5): 705~714
38. Holder JW, Ulrich JC, DeBono AC, Godfrey PA, Desjardins CA, Zucker J, Zeng Q, Leach AL, Ghiviriga I, Dancel C, Abeel T, Gevers D, Kodira CD, Desany B, Affourtit JP, Birren BW, Sinskey AJ. Comparative and functional genomics of *Rhodococcus opacus* PD630 for biofuels development. *PLoS Genet*, 2011, 7(9): e1002219
39. Kalscheuer R, Arenskotter M, Steinbuchel A. Establishment of a gene transfer system for *Rhodococcus opacus* PD630 based on electroporation and its application for recombinant biosynthesis of poly(3-hydroxyalkanoic acids). *Appl Microbiol Biotechnol*, 1999, 52(4): 508~515
40. Alvarez HM, Mayer F, Fabritius D, Steinbuchel A. Formation of intracytoplasmic lipid inclusions by *Rhodococcus opacus* strain PD630. *Arch Microbiol*, 1996, 165(6): 377~386

# 原核生物 Dynamin 蛋白家族的功能与进化

耿丹丹[1,2]，Simon Cichello[3]，张少强[1]，陈 勇[2]

1. 天津师范大学计算机与信息工程学院，天津 300387；
2. 中国科学院生物物理研究所生物大分子国家重点实验室，北京 100101；
3. *School of Life Sciences, La Trobe University, Melbourne, Victoria 3086, Australia*

**收稿日期**：2013-07-28；**接受日期**：2013-09-01
**基金项目**：国家自然科学基金项目(61273228，61103073)，天津市科委自然科学基金项目(11JCYBJC26600)
**通讯作者**：张少强，电话：(022)23766027，E-mail：sqzhang@163.com
陈勇，电话：(010)64888521，E-mail：yongchen@tsinghua.edu.cn

**摘要**：细胞膜系统的动态变化是原核与真核细胞中多种细胞功能实现的基础。在真核细胞中，膜的融合与分裂过程是由动力蛋白(dynamin)家族的 GTP 酶催化的，然而，这一机制在原核生物中却少有研究。文章总结了现有原核生物动力蛋白最新的结构和生化数据结果，探讨了它们的结构及功能特性。通过分析动力蛋白家族及其蛋白质功能域在原核生物中的进化分布，初步揭示了该蛋白家族的进化历史和功能演化，并且进一步探讨了动力蛋白参与脂滴形成和分裂过程的可能机制。基于以上研究，最后给出了动力蛋白参与脂滴动态变化的假说模型，以便于原核生物动力蛋白的功能研究。

**关键词**：动力蛋白；脂滴；功能进化；蛋白质功能域；膜动力学
**中图分类号**：Q933
**DOI**：10.3724/SP.J.1260.2013.30146